

DOI: 10.17725/rensit.2023.15.425

Sound reflection from an elastic finite cylindrical shell of different relative lengths

Sergey L. Ilmenkov

St. Petersburg State Marine Technical University, <http://www.smtu.ru/>

St. Petersburg 190121, Russian Federation

E-mail: sl_ilmenkov@mail.ru

Sergey A. Pereselkov, Nikolay V. Ladykin

Voronezh State University, <http://www.vsu.ru/>

Voronezh 394006, Russian Federation

E-mail: pereselkov@yandex.ru, ladykin.edu@yandex.ru

Vladimir I. Grachev

Kotel'nikov Institute of Radioengineering and Electronics of RAS, <http://www.cplire.ru/>

Moscow 125009, Russian Federation

E-mail: grachev@cplire.ru

Received November 28, 2023, peer-reviewed December 01, 2023, accepted December 03, 2023, published December 06, 2023.

Abstract: A calculation of the sound pressure frequency dependences scattered by a finite elastic cylindrical shell placed in a liquid medium is presented. The shell has hemispherical ends and is considered either hollow or filled with gas or liquid. The scattered sound pressure under conditions of hydroelastic contact on the shell surfaces is found by jointly using the Kirchhoff integral and the integral equation for the elastic medium displacement vector, obeying the Lamé equation. Boundary conditions regarding stresses and displacements are formulated for each of the shell contact surfaces with the external and internal environments. Considering approach is based on the numerical transformation of continuous integral equations into a system of linear algebraic equations using curvilinear isoparametric boundary elements. In this case, the elements geometry and the main variables (displacements and stresses) are specified using the same interpolating relations (shape functions). The scattered sound pressure frequency dependences are calculated and analyzed for various ratios of the length and shell diameter.

Keywords: finite elastic cylindrical shell, Kirchhoff integral equation, displacement vector, boundary elements, scattered sound pressure

UDC 534.26

Acknowledgments: The study was supported by the Russian Science Foundation grant No. 23-61-10024, <https://rscf.ru/project/23-61-10024/>.

For citation: Sergey L. Ilmenkov, Sergey A. Pereselkov, Vladimir I. Grachev, Nikolay V. Ladykin. Sound reflection from an elastic finite cylindrical shell of different relative lengths. *RENSIT: Radioelectronics. Nanosystems. Information Technologies*, 2023, 15(4):425-432e. DOI: 10.17725/rensit.2023.15.425.

CONTENTS

1. INTRODUCTION (426)

2. PROBLEM STATEMENT (426)

3. RESULTS OF SOUND REFLECTION CHARACTERISTICS NUMERICAL ANALYSIS (429)

4. CONCLUSION (431)
REFERENCES (431)

1. INTRODUCTION

It is known that the target detection range of modern sonar systems significantly depends on the energy losses of probing and reflected signals. The increase in such losses with frequency dictates the need to reduce the location signal frequency. In addition, discrete signal components in the low-frequency range are less sensitive to fluctuations in the marine environment parameters and are very informative in identifying individual characteristics of objects. In the context of the principles of a deformable solid mechanics, it is possible to obtain solutions to boundary value problems for objects of non-analytical shape using numerical methods: finite differences, T-matrices, finite and boundary elements. Algorithms based on these methods form the basis of common software packages for solving boundary value problems (ANSYS, NASTRAN, COSMOS/M, COMSOL Multiphysics [1-5], etc.).

With all the undoubted advantages of such packages, specially developed individual software can have significant advantages in practice, having: compactness, speed, uniqueness, interaction with analytical and approximate approaches, accessibility, absence of an expensive license, etc. The solution presented in this article is based on the use of a boundary integral equation with respect to unknown surface displacements and stresses, interpolated by identical polynomial functions through their values at the nodal points of curvilinear isoparametric boundary elements. The calculation algorithm implementation was carried out using software specially developed by the author.

2. PROBLEM FORMULATION

The sound pressure p_s scattered by an elastic body can be found using the Kirchhoff integral and the Green's function for free space, which is the point source field placed at a far-field point [6-9]:

$$p(\mathbf{r}_1) = \frac{1}{4\pi} \int_S [p(\mathbf{r}_0) \frac{\partial}{\partial n} G(\mathbf{r}_1; \mathbf{r}_0) - \frac{\partial}{\partial n} p(\mathbf{r}_0) G(\mathbf{r}_1; \mathbf{r}_0)] dS, \quad (1)$$

where $p(\mathbf{r}_1)$ is the sound pressure in the far field of the object (Fraunhofer zone); \mathbf{r}_1 – radius vector of the far field point; S – closed surface surrounding an object with a continuous external normal \mathbf{n} ; $p(\mathbf{r}_0)$ and $\partial p(\mathbf{r}_0)/\partial n$ – amplitude-phase distributions of sound pressure and its gradient on the surface S ; \mathbf{r}_0 – radius vector of a point on the surface S ; $G(\mathbf{r}_1; \mathbf{r}_0)$ is the Green's function satisfying the inhomogeneous Helmholtz equation.

The transition from ideal boundary conditions on the diffuser surface to the conditions of hydroelastic contact adds to (1) the integral equation for the displacement vector \mathbf{u} and the boundary conditions for contact of an ideal compressible fluid with an elastic medium [10-12]:

$$\mathbf{u} = \iint_S \{ \mathbf{t}(\mathbf{r}_0) G_t(\mathbf{r}; \mathbf{r}_0) - \mathbf{u}(\mathbf{r}_0) [\mathbf{n} \cdot \Sigma(\mathbf{r}; \mathbf{r}_0)] \} dS, \quad (2)$$

where $\mathbf{t}(\mathbf{r}_0) = \mathbf{nT}(\mathbf{r}_0)$ – voltage vector; \mathbf{n} is the unit vector of the external normal to S ; $\mathbf{T}(\mathbf{r}_0)$ – stress tensor of an isotropic material; $G_t(\mathbf{r}; \mathbf{r}_0)$ – Green's displacement tensor; $\Sigma(\mathbf{r}; \mathbf{r}_0)$ – Green's stress tensor.

In equation (2), the stress vectors $\mathbf{t}(\mathbf{r}_0)$ and displacement $\mathbf{u}(\mathbf{r}_0)$ on the surface of the body S are unknown, and in equation (1) in this case, $p(\mathbf{r}_0)$ and $\partial p(\mathbf{r}_0)/\partial n$ on the same surface are unknown. The displacement vector of the elastic medium \mathbf{u} , with a harmonic dependence on time, obeys the Lamé equation and can be represented, as

is known, as a combination of scalar and vector potentials [12].

The following boundary conditions must be satisfied on the surfaces of the shell, based on the complete system of equations of the linear theory of elasticity, which determines the state of dynamic equilibrium of the elastic body [11,12]:

1) the normal component of the displacement vector u_n is continuous and related to the normal derivative of the diffracted pressure $p_\Sigma = p_i + p_s$ (p_i is the sound pressure in the incident wave):

$$u_n = (1/\rho_0\omega^2)(\partial p_\Sigma / \partial n)|_s, \tag{3}$$

where ρ_0 is the density of the liquid medium, kg/m³; $\omega = 2\pi f$, f – sound signal frequency, Hz;

2) normal stress σ_n :

– on the outer surface of the shell is equal to the acoustic pressure in the liquid

$$\sigma_n|_s = p_\Sigma, \tag{4}$$

- on the inner surface of the shell it is either absent (hollow shell) or equal to the sound pressure of the gaseous or liquid filler;

3) there are no tangential stresses:

$$\tau_i|_s = 0. \tag{5}$$

Using (3)-(5), one group of unknowns on S can be eliminated from equations (1) and (2), and the two remaining unknowns can be found from a joint solution of these equations [12,13].

The approach under consideration is based on the numerical transformation of continuous integral equations (1) and (2) into a system of linear algebraic equations using quadratic isoparametric elements. The use of curved boundary elements provides a more detailed discretization of the boundary surface and increases the accuracy of the result while reducing computation time. When constructing a mesh of boundary elements, the sampling step Δ of the surface S in the direction of any of the coordinates should not exceed $(0.25 \div 0.5) \cdot \lambda_0$ (λ_0 is the length of the sound wave in the liquid). Near the edges and corners of the surface, the calculation algorithm provides for condensation of nodal points with a decrease in the sampling step up to values $\Delta \sim (0.025 \div 0.05) \cdot \lambda_0$. With such discretization, the three-dimensional boundary of the region S is divided into triangular and quadrangular elements (**Fig. 1**), at the nodes of which some coefficients are specified, and the continuous integrand function is approximately represented as a series of basic (interpolating) shape functions multiplied by these coefficients. The nodal coordinates of any point of the original elements x_{i_u} are transformed into the corresponding curvilinear coordinates x_i ($i = 1, 2, 3$), and the geometry of the element $x_i(\xi)$, displacement $u_i(\xi)$ and stress $t_i(\xi)$ are specified using the same shape functions [12,13].

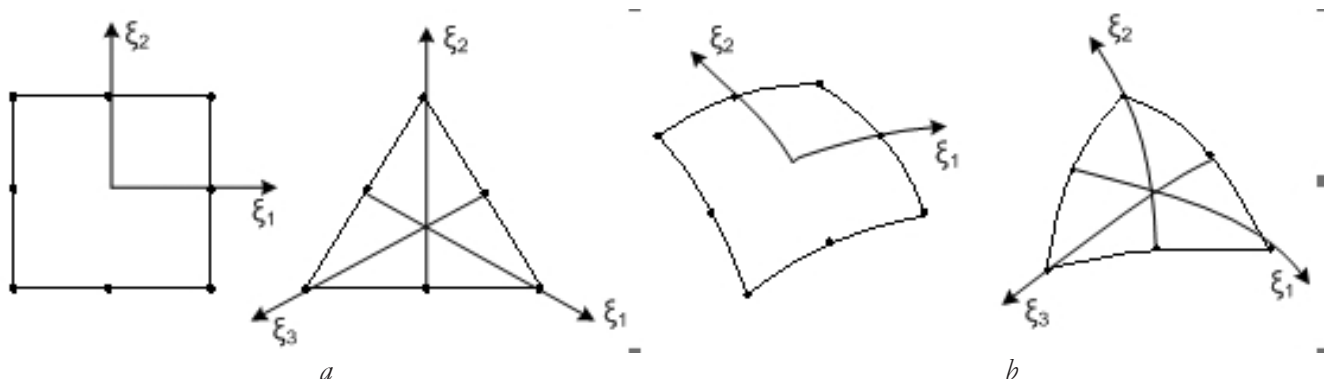


Fig. 1. Initial flat (a) and corresponding curvilinear isoparametric (b) boundary elements

Using such relations allows us to obtain the matrix equation based on (2):

$$[H]\{u\} = [\tilde{G}]\{t\}, \tag{6}$$

where H and \tilde{G} are matrices of coefficients obtained as a result of numerical integration.

Integral (1) will take the form [11-13]:

$$p_s(P) = \frac{1}{4\pi} \int_S [p_\Sigma(Q) \frac{\partial}{\partial n} (e^{ikr}/r) - (e^{ikr}/r) \rho_0 \omega^2 (\mathbf{u} \cdot \mathbf{n})] dS + 4\pi p_i(P), \tag{7}$$

where $p_\Sigma(Q)$ is the diffracted sound pressure at point Q of the surface S .

Having performed numerical integration (7) and expressing part of the unknown stresses in (6) in terms of pressure in accordance with the boundary condition (4), we obtain:

$$[T]\{u\} = [D]\{p_\Sigma\} + 4\pi\{p_\Sigma\}, \tag{8}$$

$$[H]\{u\} = [G]\{t\} + F\{p_\Sigma\}, \tag{9}$$

where T, D, G and F are coefficient matrices.

Next, from equations (6) and (8), the distributions $p_\Sigma(Q)$ and $(\mathbf{u} \cdot \mathbf{n})$ on the surface S are found, and then, based on (7), $p_\Sigma(P)$ in a liquid medium is determined using quadrature formulas.

Let us consider the practical implementation of this approach in relation to an isotropic circular cylindrical shell of length L and thickness b , limited at the

ends by hemispheres of radius a at different values of the relative length L/a (**Fig. 2**):

We will assume that the shell is thin ($b/a \leq 0.05$). As is known, for such shells it is possible, based on the Kirchhoff–Love hypothesis, to move from three-dimensional relations of the theory of elasticity to two-dimensional ones. In this case, the exclusion of tangential and shear forces allows, when describing small bending vibrations of the shell, to use a system of two differential equations and determine the projections of all forces and stresses on the direction of the normal to the middle surface of the shell (the wave vector \mathbf{k} is perpendicular to the z -axis of the cylinder).

Let us introduce coordinate systems associated with each part of the surface S , for which, at $\theta_0 = 90^\circ$, all the main physical variables are functions of only two coordinates, so the displacement vector will also have two components. For the cylindrical part of the surface S_2 they will have the form [9,14]:

$$u_r = -\frac{\partial \Phi}{\partial r} + \frac{1}{r} \frac{\partial \Psi}{\partial \varphi}; \quad u_\varphi = -\frac{1}{r} \frac{\partial \Phi}{\partial \varphi} - \frac{\partial \Psi}{\partial r}. \tag{10}$$

Using the representations of the strain components $\epsilon_r, \epsilon_\varphi$ through the components of the displacement vector, as well as the generalized Hooke’s law for an isotropic medium, it is possible to express the elastic stresses on the surface S_2 through the scalar Φ and vector Ψ potentials [12,15]:

$$\left. \begin{aligned} \sigma_r &= \lambda \mathcal{G} + 2\mu \epsilon_r = \lambda k_1^2 \Phi + \left(-\frac{\partial^2 \Phi}{\partial r^2} - \frac{1}{r^2} \frac{\partial \Psi}{\partial \varphi} + \frac{1}{r} \frac{\partial^2 \Psi}{\partial r \partial \varphi} \right), \\ \tau_{r\varphi} &= 2\mu \gamma_{r\varphi} = \mu \left(-\frac{2}{r} \frac{\partial^2 \Phi}{\partial r \partial \varphi} + \frac{2}{r^2} \frac{\partial \Phi}{\partial \varphi} - k_2^2 \Psi - 2 \frac{\partial^2 \Psi}{\partial r^2} \right). \end{aligned} \right\} \tag{11}$$

where r, φ – cylindrical coordinates of point Q ; $\mathcal{G} = \epsilon_r + \epsilon_\varphi = \text{div} \mathbf{u}$; k_1 and k_2 are the wave numbers of longitudinal and transverse waves in the elastic shell material.

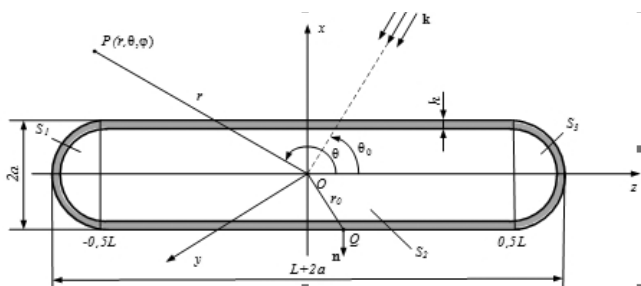


Fig. 2. Elastic finite cylindrical shell with hemispheres at the ends; S_2 is the area of the lateral surface of the cylinder, S_1 and S_3 are the surface areas of the hemispheres.

Similar relations for the hemispherical parts of the shell S_1 and S_3 will have the form:

$$\left. \begin{aligned} u_r &= -\frac{\partial\Phi}{\partial r} + \frac{1}{r} \text{ctg}\theta \Psi + \frac{1}{r} \frac{\partial\Psi}{\partial\theta}; \\ \sigma_r &= \lambda\vartheta + 2\mu\varepsilon_r = \lambda k_1^2 \Phi + \\ &+ 2\mu \left(-\frac{\partial^2\Phi}{\partial r^2} + \frac{1}{r} \text{ctg}\theta \frac{\partial\Psi}{\partial r} - \frac{1}{r^2} \text{ctg}\theta \Psi + \frac{1}{r} \frac{\partial^2\Psi}{\partial r \partial\theta} - \frac{1}{r^2} \frac{\partial\Psi}{\partial\theta} \right); \\ \tau_{r\theta} &= 2\mu\gamma_{r\theta} = \\ &= \mu \left(\frac{1}{r^2} \text{ctg}\theta \frac{\partial\Psi}{\partial\theta} + \frac{1}{r^2} \frac{\partial^2\Psi}{\partial\theta^2} - \frac{\partial^2\Psi}{\partial r^2} - \frac{2}{r^2} \frac{\partial\Phi}{\partial\theta} - \frac{1}{r^2 \sin^2\theta} \Psi \right); \end{aligned} \right\} (12)$$

where r, θ – spherical coordinates of point Q ; $\vartheta = \varepsilon_r + \varepsilon_\theta = \text{div}\mathbf{u}$.

Substituting relations for the components of the displacement vector and elastic stresses into the boundary conditions (3)-(5), we obtain for each point Q of the surface S a system of algebraic equations for finding unknown coefficients in the expansions of elastic potentials, and then we find the distributions $p_\Sigma(Q)$ and u_r at the boundary element nodes (points Q) on the surface S .

3. RESULTS OF NUMERICAL ANALYSIS OF CHARACTERISTICS SOUND REFLECTIONS

Let us consider the main results of calculations of the frequency characteristics

$$lg|p_\Sigma(P)|, \text{ dB}$$

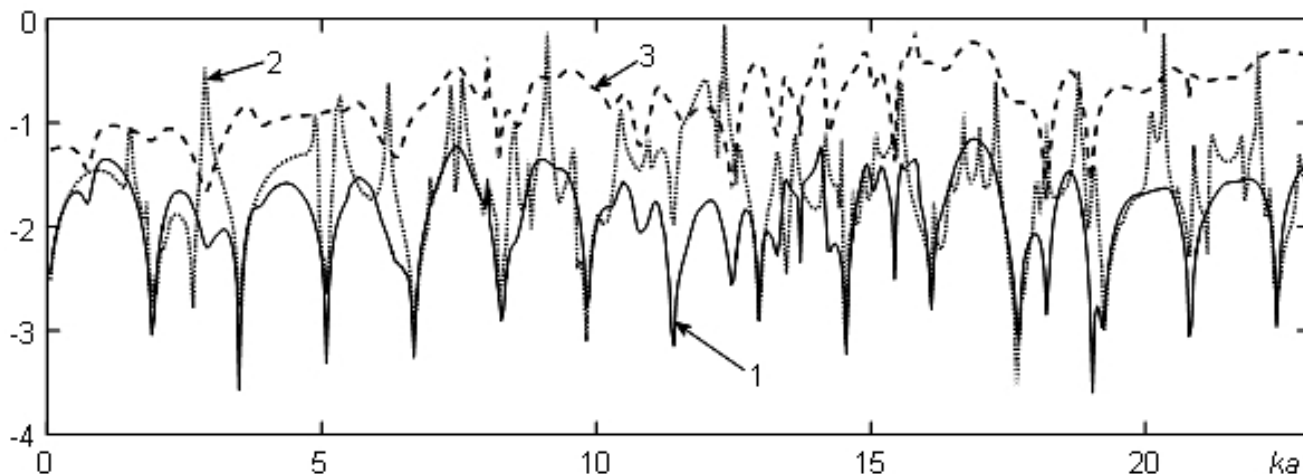


Fig. 3. Levels of modulus of frequency dependences of an audio signal reflected by a shell filled with: air (1), water (2) and vacuum (3) at $\theta = 90^\circ$; $L/a = 20$; $b/a = 0.01$.

of sound reflection by a steel shell of the shape under consideration in the range of wave radii $ka = 0.95 \div 25.0$. Fig. 3 shows the frequency dependences of the modulus levels $p_\Sigma(P)$ at traverse location ($\theta_0 = 90^\circ$) for a shell filled with air (curve 1), water (curve 2) and vacuum (curve 3). The geometric parameters of the shell are: $L/a = 20$; $b/a = 0.01$.

As can be seen from the figure, the levels of modules $p_\Sigma(P)$ for a hollow shell exceed the corresponding values for an air-filled shell on average over the range by 1...1.5 dB ($\approx 20\% \dots 50\%$). For a shell filled with water, the added mass can lead to the interaction of vibration modes and, accordingly, to an increase in the likelihood of resonance phenomena occurring. The latter can also be determined by the propagation of Scholte-Stoney type waves in the liquid and elastic waves of the Lamb type in the shell material [11,12,14], which is observed mainly for $ka > 3$. The values of the resonant frequencies are determined by the integer number of lengths of these half-waves, which fit along the closed contour of the shell. In the presence of a liquid filler, the probability of phase matching for such half-waves at the excitation point increases.

$\lg|p_{\Sigma}(P)|, \text{ dB}$

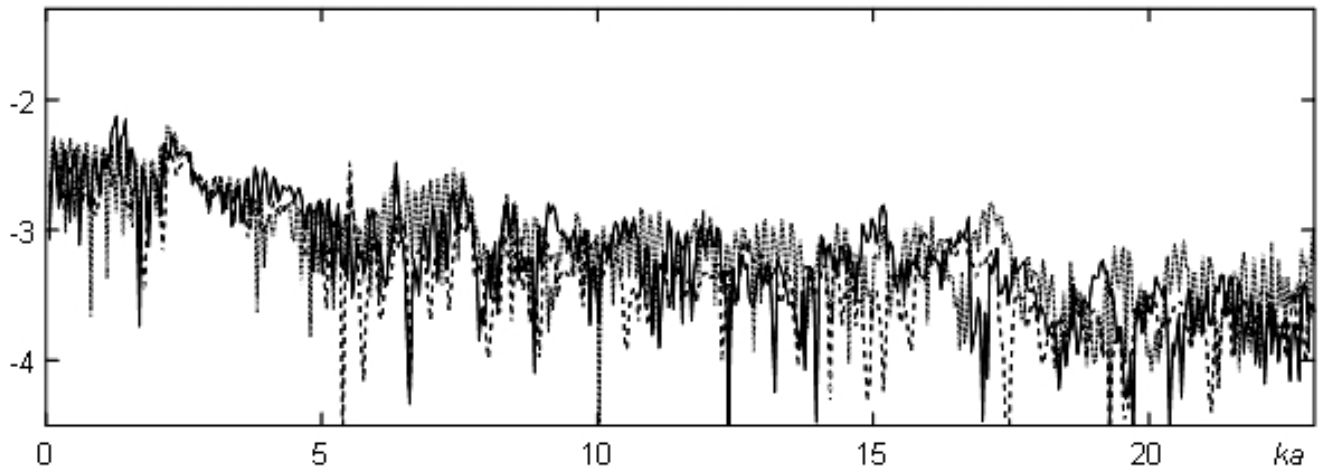


Fig. 4. Levels of modules of frequency dependences of an audio signal reflected by a shell filled with air, at $L/a = 20$; $-\theta_0 = 0^\circ$; $-\theta_0 = 30^\circ$; $-\theta_0 = 60^\circ$.

In addition, in this case, compared to an air-filled shell, at a number of resonant frequencies ($ka \approx 5-10, 17-22$, etc.) there is a tendency to double the frequency spectrum of the reflected signal. Lower in frequency ($ka \leq 3$) spatial coincidence resonances may occur.

Figures 4-7 show the frequency dependences of $\lg|p_{\Sigma}(P)|, \text{ dB}$ for location angles $\theta_0 = 0^\circ; 30^\circ; 60^\circ$ of a shell filled with air, at $b/a = 0.01$ and relative elongations $L/a = 20; 10; 5$ and 2 .

The presented results show that at non-averse location angles, the levels of the reflected signal are generally 1...2 dB lower than at $\theta_0 = 90^\circ$. When L/a decreases by a factor of two, the repetition frequency of elastic resonances caused by the rounding of the shell contour by waves of the Scholte-Stoneley and Lamb type decreases by a factor of 2...3. When $L/a < 10$, the role of spatial coincidence resonances increases (up to $\approx 30\% \dots 50\%$), which manifest themselves predominantly in the range $ka < 2$ and location angles $\theta_0 = 30^\circ, 60^\circ$.

$\lg|p_{\Sigma}(P)|, \text{ dB}$

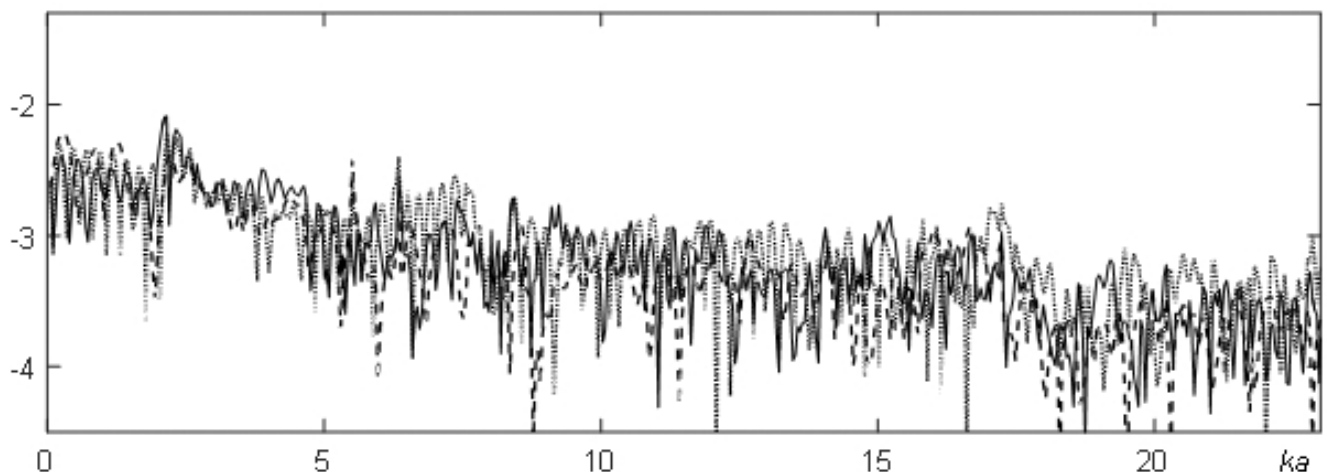


Fig. 5. Levels of modules of frequency dependences of an audio signal reflected by a shell filled with air, at $L/a = 10$; $-\theta_0 = 0^\circ$; $-\theta_0 = 30^\circ$; $-\theta_0 = 60^\circ$.

$\lg|p_{\Sigma}(P)|, \text{ dB}$

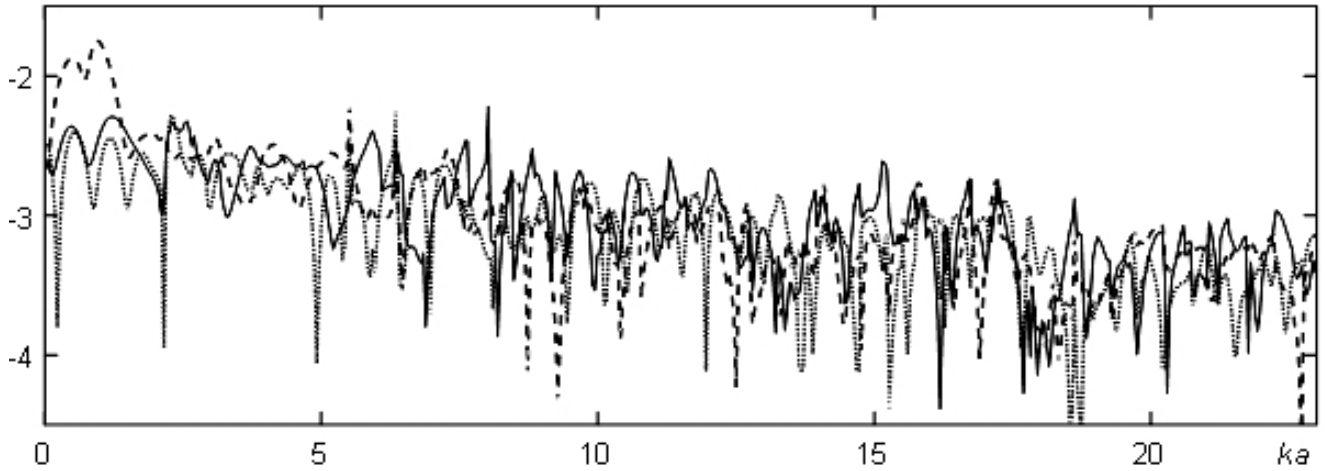


Fig. 6. Levels of modules of frequency dependences of an audio signal reflected by a shell filled with air, at $L/a = 5; -\theta_0 = 0^\circ; -\theta_0 = 30^\circ; -\theta_0 = 60^\circ$.

4. CONCLUSION

The use of a numerical transformation of continuous integral equations into a system of linear algebraic equations for unknown displacements and stresses, determined by their values at the nodal points of curvilinear boundary elements, made it possible to calculate the levels of sound pressure dissipated by a finite elastic cylindrical shell. The latter has hemispherical ends, is placed in a liquid medium and is considered both hollow and filled with gas or liquid. The scattered sound pressure on the surfaces

of the shell is found by combining the Kirchhoff integral and the integral equation for the displacement vector of the elastic medium, which obeys the Lamé equation. The frequency dependences of the modulus levels of a stationary sound signal reflected by the shell are calculated and analyzed at various location angles, relative elongations, and options for filling its internal volume. The implementation of the calculation algorithm was carried out using software specially developed by the author

$\lg|p_{\Sigma}(P)|, \text{ dB}$

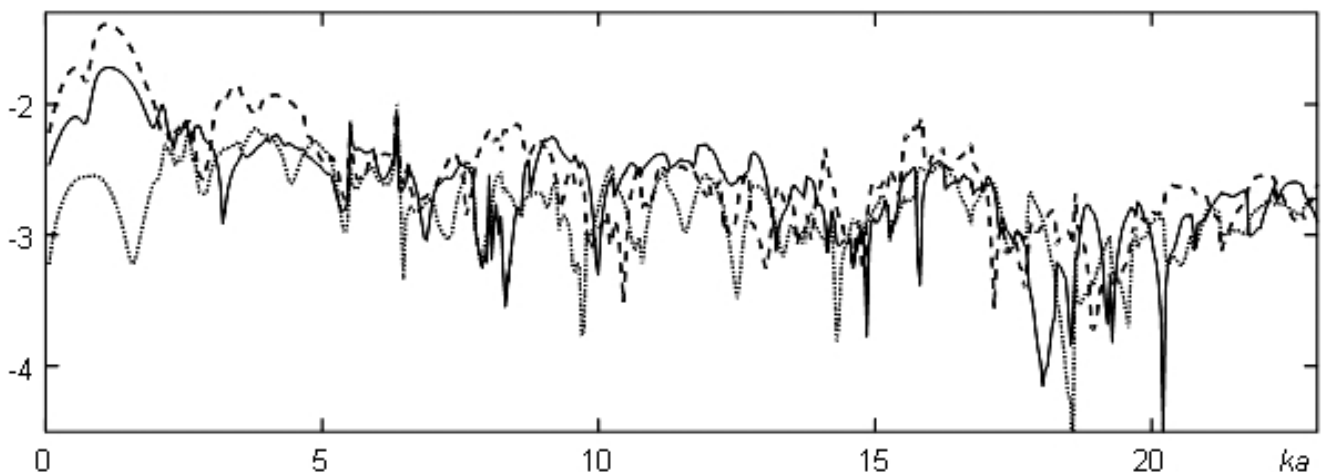


Fig. 7. Levels of modules of frequency dependences of an audio signal reflected by a shell filled with air, at $L/a = 2; -\theta_0 = 0^\circ; -\theta_0 = 30^\circ; -\theta_0 = 60^\circ$.

REFERENCES

1. Kudin MV. *Solving acoustics problems in the ANSYS software package: an electronic manual*. Nizhny Novgorod, Nizhny Novgorod State University, 2011, 27 p.
2. A.SYS 11.0. Documentation. Theory Reference for ANSYS and ANSYS Workbench. Acoustics// ANSYS, Inc. Southpointe Technology Drive Canonsburg, 2004, 1067 p.
3. Shatrov BV, Bukharov SA, Martynenko YUR, et al. *General-purpose finite element analysis system MSC Nastran: methodological manual*. Moscow, MSC Software Corporation, 2020, 50 p.
4. Shimkovich DG. *Structural analysis in MSC Nastran: methodological manual*. Moscow, DMK Press, 2003, 448 p.
5. Krasnikov GE, Nagornov OV, Starostin NV. *Modeling physical processes using the Comsol Multiphysics package: a methodological manual*. Moscow, MEPHI Publishing House, 2012, 184 p.
6. Ilmenkov SL. On the application of the Green's function method for calculating sound fields. *Proceedings of the IV Far Eastern Acoustic Conference*, p. 73-75. Vladivostok, Publishing house of the Far Eastern Polytechnic Institute, 1986.
7. Ilmenkov SL. On the accuracy of the Green's function method for calculating sound fields of radiators of complex shape. *Abstracts of reports of the All-Union meeting-seminar "Deep-sea systems and complexes."* Part 1, p.75. Cherkassy, 1986.
8. Ilmenkov SL. Green's function method in the problem of sound diffraction on bodies of non-analytical shape. *Marine Intelligent Technologies*, 2014, 2:32-36.
9. Shenderov EL. *Radiation and scattering of sound*. Leningrad, Sudostroenie Publ., 1989, 301 p.
10. Brebbia K, Walker S. *Application of the boundary element method in engineering*. Moscow, Mir Publ., 1981, 248 p.
11. Ilmenkov SL. Solving the problem of sound diffraction on an elastic body of non-analytical shape using the boundary element method. *Marine Intelligent Technologies*, 2015, 1, 1(27):30-36.
12. Kleshchev AA. *Hydroacoustic diffusers*. St. Petersburg, Sudostroenie Publ., 1991, 248 p.
13. Seybert AF, Wu TW, Wu XF. Radiation and Scattering of acoustic waves from elastic solids and shells using the boundary element method. *Journal of the Acoustical Society of America*, 1988, 84(I.5)1906-1911.
14. Kleshchev AA, Klyukin II. *Fundamentals of hydroacoustics*. Leningrad, Sudostroenie Publ., 1987, 224 p.
15. Ilmenkov SL. *Development of methods for solving boundary problems of hydroacoustics*. St. Petersburg, St. Petersburg State Medical University, 2020, 190 p.